Available online at www.sciencedirect.com
SCIENCE DIRECT
Virology 352 (2006) 157–168
VIROLOGY
www.elsevier.com/locate/yviro

Characterization of the CD8$^+$ T cell responses directed against respiratory syncytial virus during primary and secondary infection in C57BL/6 mice

Michaël V. Lukens [a], Erwin A.W. Claassen [b], Patricia M.A. de Graaff [a], Mariska E.A. van Dijk [a], Peter Hoogerhout [c], Mireille Toebes [d], Ton N. Schumacher [d], Robbert G. van der Most [b], Jan L.L. Kimpen [a], Grada M. van Bleek [a,*]

[a] *Department of Pediatrics, The Wilhelmina Children's Hospital, University Medical Center, KE.04.133.1, Lundlaan 6, 3584 EA Utrecht, The Netherlands*
[b] *Department of Immunology, Faculty of Veterinary Science, University of Utrecht, Utrecht, The Netherlands*
[c] *National Vaccine Institute, Bilthoven, The Netherlands*
[d] *Division of Immunology, The Netherlands Cancer Institute, Amsterdam, The Netherlands*

Received 16 January 2006; returned to author for revision 27 February 2006; accepted 18 April 2006
Available online 30 May 2006

Abstract

The BALB/c mouse model for human respiratory syncytial virus infection has contributed significantly to our understanding of the relative role for CD4$^+$ and CD8$^+$ T cells to immune protection and pathogenic immune responses. To enable comparison of RSV-specific T cell responses in different mouse strains and allow dissection of immune mechanisms by using transgenic and knockout mice that are mostly available on a C57BL/6 background, we characterized the specificity, level and functional capabilities of CD8$^+$ T cells during primary and secondary responses in lung parenchyma, airways and spleens of C57BL/6 mice. During the primary response, epitopes were recognized originating from the matrix, fusion, nucleo- and attachment proteins, whereas the secondary response focused predominantly on the matrix epitope. C57BL/6 mice are less permissive for hRSV infection than BALB/c mice, yet we found CD8$^+$ T cell responses in the lungs and bronchoalveolar lavage, comparable to the responses described for BALB/c mice.
© 2006 Elsevier Inc. All rights reserved.

Keywords: Respiratory syncytial virus; C57BL/6; CD8$^+$ T cells; Inactivation; Tetramer

Introduction

Respiratory syncytial virus (RSV), a member of the family of Paramyxoviridae, is the leading cause of viral lower respiratory tract infection in early childhood. Although about 50 years have elapsed since the virus was discovered, the essential parameters that determine a severe disease course during primary infection have not been unambiguously identified. Besides the burden RSV infections pose on the population during primary disease, which is usually attracted during the first year of life, the virus also causes recurrent reinfections which are a main health concern in elderly people and immune compromised individuals (Falsey et al., 2005). Moreover, RSV lower respiratory tract disease is followed by recurrent episodes of wheezing in a considerable population of children (Bont et al., 2004). A safe and effective vaccine is not available. A dramatic vaccine trial was performed in the 1960s with formalin inactivated RSV (FI-RSV). Vaccinees in this trial developed enhanced disease upon exposure to the natural virus (Kim et al., 1969; Chin et al., 1969). For the development of future vaccines that are highly protective and safe, two essential points need to be addressed. First, how can immune-mediated enhancement of disease be prevented? And second, why is immunity incomplete after natural RSV infection and how can this be improved by a vaccine?

Several aspects of the immune response against RSV including the enhanced disease mechanism after FI-RSV vaccination have been extensively studied in mouse models,

* Corresponding author. Fax: +31 30 2505349.
E-mail address: g.vanbleek@umcutrecht.nl (G.M. van Bleek).

0042-6822/$ - see front matter © 2006 Elsevier Inc. All rights reserved.
doi:10.1016/j.virol.2006.04.023

particularly in BALB/c, a mouse strain highly permissive to hRSV infection (Prince et al., 1979; Waris et al., 1996). From these studies, it was learned that $CD4^+$ Th2 cells are a crucial component of enhanced disease characterized by an eosinophilic influx in the lungs that was also observed in FI-RSV vaccinated children (Connors et al., 1992). The effect of this Th2 response could be antagonized by an effective simultaneous $CD8^+$ T cell response, whereby high production of IFN-γ seemed crucial (Srikiatkhachorn and Braciale, 1997; Hussell et al., 1997).

Another finding in BALB/c mice was that $CD8^+$ T cells in the lung tissue were partially functionally inactivated. This conclusion was made from the observation that in the same lung-derived cell sample, the number of $CD8^+$ T cells specific for a certain viral epitope as measured by H-2 tetramer staining did not match up with the number of $CD8^+$ T cells that produced IFN-γ upon an ex vivo stimulus with the same peptide (Chang and Braciale, 2002). This discrepancy was not found in splenic cell samples but only found in lung tissue when live virus was present. The authors suggested that this functional impairment of the $CD8^+$ T cell response might have some relation with the incomplete long-term memory against RSV (Chang and Braciale, 2002). The mechanism by which $CD8^+$ T cells became inactivated is unclear. In in vitro responses with human T cells, high surface expression of the F protein on accessory cells was reported to impair the proliferative response of T cells induced by a polyclonal stimulus (Schlender et al., 2002). However, others have suggested the role of soluble factors as the cause for impaired polyclonal T cell activation in the presence of live RSV (Salkind et al., 1991; Preston et al., 1995; de Graaff et al., 2005).

Genetic factors have been shown to affect susceptibility to primary hRSV infection in mice as well as the nature of the secondary immunological response to RSV infection after vaccination (Hussell et al., 1998; Prince et al., 1979; Stark et al., 2002). MHC genes and non-MHC genes both played a crucial role in disease severity. Hence, the detailed study of T cell responses in other mice strains besides BALB/c might further our understanding of the mechanisms leading to protective immunity or immune pathology. C57BL/6 mice have been studied in various infection models in parallel to BALB/c mice. From these studies, it has become clear that for certain pathogens BALB/c mice are more prone to develop a Th2 skewed immune response whereas C57BL/6 mice elicit Th1 type responses (Sacks and Noben-Trauth, 2002; Guinazu et al., 2004; Lenzo et al., 2003). This essential difference in pathogen-specific immune responses as well as the fact that many interesting transgenic and knockout mice are available on an H-2^b background determined our choice to characterize the $CD8^+$ T cell response against RSV in the C57BL/6 mouse model.

Results

Identification of H-2^b-restricted epitopes of RSV proteins by Elispot

It has been reported that $CD8^+$ T cells in the lungs of BALB/c mice are functionally inactivated. To be able to judge whether this observation can be generalized to other mouse strains and to study the mechanism of anti-viral T cell activation using transgenic or KO mouse models, it was necessary to identify $CD8^+$ T cell epitopes in a different mouse strain. Because many interesting genetically manipulated mice are available on an H-2^b background, we initiated an epitope search in C57BL/6 mice. A panel of 18-mer peptides (12 amino-acid overlap) of the RSV-F protein as well as a set of peptides derived from other RSV proteins, predicted by algorithms for the MHC class I allele H-$2D^b$ were synthesized (Table 1) (Rammensee et al., 1999; Parker et al., 1994). We initially focused on H-$2D^b$ because it appeared to be the main restriction element during RSV infection in H-2^b mice (Hussell et al., 1998). Splenocytes from RSV-infected C57BL/6 mice were isolated 8 days after primary infection and were stimulated with the synthetic peptides. The peptides were tested for their capability to induce IFN-γ production by T cells in an Elispot assay. The number of spot-forming cells (SFC) per 10^6 cells was determined (Fig. 1). The 18-mer peptide set was initially tested as mixtures of 6 consecutive peptides, followed by tests with individual peptides of positive pools. The most dominant response in C57BL/6 was directed against the $M_{187–195}$ sequence, derived from the matrix protein. We further found substantial responses against two sequences from the Fusion protein ($F_{250–258}$ and $F_{433–450}$), one from the nucleoprotein ($NP_{360–368}$) and a response against a peptide representing amino acid residues 177–194 from the G protein ($G_{177–194}$).

Identified epitopes are recognized by $CD8^+$ T cells

Because of the length of some of the peptides, the observed responses in the Elispot assay could reflect $CD4^+$ and/or $CD8^+$ T cell responses. Therefore, intracellular cytokine staining (ICS) was performed to elucidate the role of $CD4^+$ versus $CD8^+$ T cells. Peptides that gave a strong positive result with the Elispot assay, as well as an extra peptide derived from the NP sequence that was predicted to bind to H-$2K^b$ and a shorter variant of the sequence from the G protein, were used. Peptide $F_{250–258}$ represented the nonamer contained in the two overlapping peptides $F_{241–258}$ and $F_{247–264}$ that were identified by Elispot. Lung lymphocytes from C57BL/6 mice isolated 8 days after primary infection were stimulated for 6 h with the peptides. The

Table 1
Selection of peptides tested with Elispot assay and ICS

Sequence	Protein	Predicted restriction element
NAITNAKII	$M_{187–195}$	H-$2D^b$
VVLGNAAGL	$NP_{323–331}$	H-$2D^b$
ANHKFTGL	$NP_{57–64}$	H-$2K^b$
NPKDNDVEL	$NP_{383–391}$	H-$2D^b$
NGVINYSVL	$NP_{360–368}$	H-$2D^b$
YMLTNSELL	$F_{250–258}$	H-$2D^b$
IETVIEFQQKNNRLLEIT	$F_{216–234}$	H-$2D^b$
KTFSNGCDYV	$F_{433–442}$	H-$2D^b$
SNNPTCWAICKRIPNKKP	$G_{177–194}$	H-$2D^b$
SNNPTCWAICKR	$G_{177–188}$	H-$2D^b$

Sequences in bold are peptides that induced significant IFN-γ production by $CD8^+$ T cells after in vitro stimulation.

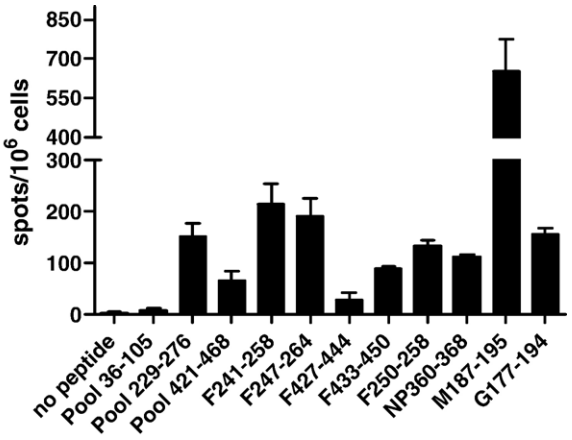

Fig. 1. Identification of immunodominant domains in RSV proteins. Mice were intranasally infected with RSV, and 8 days later splenic lymphocytes were incubated with 10 μg/ml synthetic peptides. T cells responding to synthetic peptides in the cultures were enumerated with an IFN-γ Elispot assay. The results from the positive pools, one negative pool and individual peptides are shown. Error bars represent the standard error of the mean (SEM), results are triplicate measurements of 1 mouse. An identical response pattern was observed in three individual mice. The numbers given for the pools identify the stretch of amino acid residues that is covered by the peptides in the pools.

percentage of IFN-γ producing $CD8^+$ T cells was enumerated with ICS (Figs. 2A and 5C). All responses initially detected with the Elispot assay appeared to be $CD8^+$ T cell responses. The dominant peptide $M_{187–195}$ induced 13% of the lung $CD8^+$ T cells to produce IFN-γ. Peptides derived from the NP and F proteins induced IFN-γ production, involving 2.3–8% of the lung $CD8^+$ T cells. In BALB/c mice, the lack of a G-specific $CD8^+$ T cell response after viral infection has been well documented (Srikiatkhachorn and Braciale, 1997; Alwan et al., 1994). Interestingly, we found that the response against the peptides derived from the G protein were like the other responses also $CD8^+$ T cell mediated, with 8% of the $CD8^+$ T cells in lung responding to the $G_{177–194}$ peptide. To confirm a true $CD8^+$ T cell response and determine the restriction element for this $G_{177–194}$-specific response, we performed ICS in the presence of blocking antibodies specific for H-$2D^b$ and H-$2K^b$. Furthermore, some samples were pre-incubated with an excess of the Influenza $NP_{366–374}$ or VSV $NP_{52–59}$ peptides, well-known binders for H-$2D^b$ and H-$2K^b$, respectively. The incubation of $CD8^+$ T cells with the anti-D^b antibody or competition with the influenza $NP_{366–374}$ peptide reduced the IFN-γ production by the $G_{177–194}$ peptide to near background levels, whereas pre-incubation with anti-K^b or the VSV $NP_{52–59}$ had no effect on the $G_{177–194}$-induced IFN-γ production (Fig. 2B). This result proved that the observed IFN-γ production stimulated by $G_{177–194}$ was a genuine $CD8^+$ T cell response.

The $M_{187–195}$-specific primary $CD8^+$ T cell responses in the lungs at day 8 post-infection

In BALB/c mice, it has been shown that the pulmonary RSV-specific $CD8^+$ T cell responses display a partially inactivated phenotype (Chang and Braciale, 2002; Chang et al., 2001). To determine whether a similar phenomenon happened in RSV-infected C57BL/6 mice, we compared $M_{187–195}$ tetramer and intracellular IFN-γ staining. Lung lymphocytes were stained with an $M_{187–195}$ tetramer and antibodies specific for the activation markers CD11a and CD62L or NKG2a. These antibodies were used to estimate the total number of recently activated T cells present in the sample. In the lung tissue of C57BL/6 mice undergoing a primary RSV infection, 46% of the $CD8^+$ T cells were activated as measured by up-regulation of NKG2a expression (Fig. 2C; Table 2). This was similar to the percentage of $CD8^+$ T cells that had a $CD11a^{hi}$ and $CD62L^{low}$ phenotype (49%). In MOCK-infected mice, only 4.5% (average 3.1 ± 0.9%) of the $CD8^+$ T cells in the lung had an activated phenotype.

$M_{187–195}$ tetramer staining revealed that 13% (12% average, Table 3) of the $CD8^+$ T cells in the lung stained positive (Fig. 2D). The background staining was only 0.27% in a MOCK-infected mouse and 0.29% in a mouse going through a primary influenza infection confirming the specificity of the tetramer. In influenza-infected control mice, $CD8^+$ T cells stained positive (11%) with an influenza $NP_{366–374}$ tetramer, which showed that these mice had been properly infected. The $M_{187–195}$-specific response involved 28% of the $CD11a^{hi}/CD62L^{low}$ population of $CD8^+$ T cells in the lung tissue. Fig. 2E shows that virtually all tetramer-positive cells indeed had the activated phenotype ($CD11a^{hi}$, $CD62L^{low}$, $NKG2A^{pos}$). Thus, our data clearly showed that the number of tetramer-positive cells was similar to the number of cells that produced IFN-γ after in vitro stimulation with the peptide (Table 3). Hence, in the C57BL/6 mouse strain, at day 8 after primary infection, we did not observe the discrepancy found by Chang and Braciale (2002) between the number of tetramer-positive and the number of functional cells.

Transition of $CD8^+$ T cells from effector to memory cells in the lungs

To evaluate the possible inactivation of M-specific $CD8^+$ T cells during the transition of effector phase to the early memory phase, we removed lung lymphocytes from mice 21 days p.i. and stimulated these cells with the same epitopes used at day 8 p.i. The total number of T cells recovered from the lungs at day 21 was twofold lower than at day 8. The percentage of $CD8^+$ T cells that produced IFN-γ also declined. The $M_{187–195}$ peptide still was the dominant epitope, with 5% of the $CD8^+$ T cells producing IFN-γ. The other peptides induced IFN-γ production that hardly reached above background levels (Figs. 3A and 5C). To study the activation status of these cells at this time point, we stained the cells with the activation markers and the $M_{187–195}$ tetramer. There was a decline in the percentage of activated $CD8^+$ T cells, with about 38% (33% average in the group; Table 2) $CD8^+$ T cells remaining $CD11a^{hi}$, $CD62L^{low}$. About 35% (28% average in the group; Table 2) of the $CD8^+$ T cells also remained $NKG2a^{pos}$ (Fig. 3B). Of the lung lymphocytes, 8.5% of the $CD8^+$ T cells stained positive with the $M_{187–195}$ tetramer (Fig. 3C; Table 3). Thus, at this time point we found a discrepancy between the cells able to produce IFN-γ and the cells that stained positive with the tetramer indicating

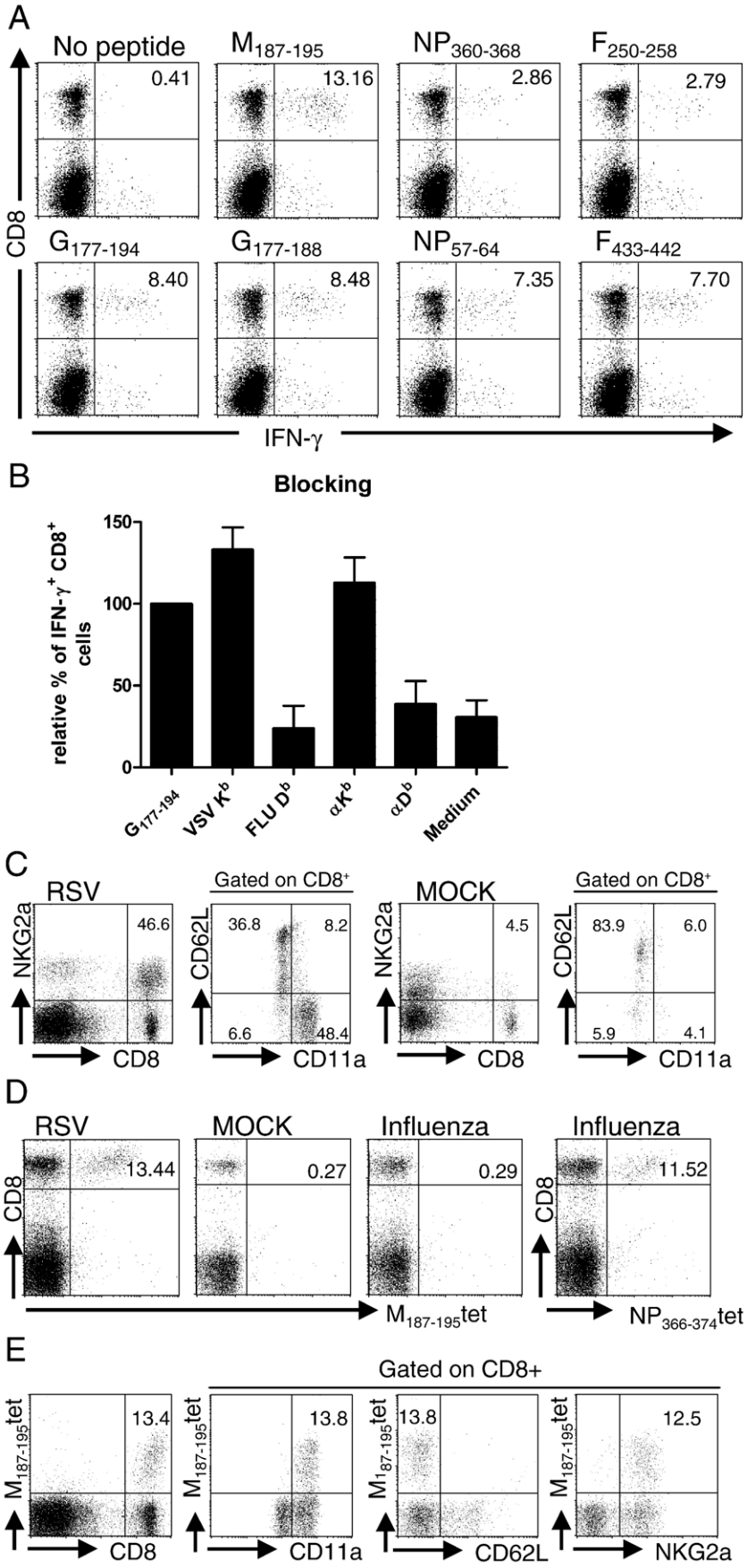
A
No peptide
M187-195
NP360-368
F250-258
0.41
13.16
2.86
2.79
CD8
G177-194
G177-188
NP57-64
F433-442
8.40
8.48
7.35
7.70
IFN-γ
B
Blocking
relative % of IFN-γ+ CD8+ cells
150
100
50
0
G177-194
VSV Kb
FLU Db
αKb
αDb
Medium
C
RSV
Gated on CD8+
MOCK
Gated on CD8+
NKG2a
46.6
CD62L
36.8
8.2
6.6
48.4
NKG2a
4.5
CD62L
83.9
6.0
5.9
4.1
CD8
CD11a
CD8
CD11a
D
RSV
MOCK
Influenza
Influenza
CD8
13.44
0.27
0.29
11.52
CD8
M187-195tet
NP366-374tet
E
Gated on CD8+
M187-195tet
13.4
13.8
13.8
12.5
CD8
CD11a
CD62L
NKG2a

Table 2
C57BL/6 mice were intranasally infected with 2.5×10^6 p.f.u. RSV A2

	Lung parenchyma		Lung airways	
	% NKG2a^{pos}	% CD11a^{hi}/ CD62^{low}	% NKG2a^{pos}	% CD11a^{hi}/ CD62^{low}
Day 8	46.4 ± 2.1	49.0 ± 0.3	69.3 ± 2.6	81.2 ± 2.7
Day 21	28.4 ± 2.5[a]	32.9 ± 5.9[a]	81.7 ± 2.5[a]	20.4 ± 2.6[a, b]

Lymphocytes obtained from the lung parenchyma and lung airways (of 4 mice per group from 2 independent experiments) at indicated time points after infection were stained with anti-CD8, anti-NKG2a or anti-CD11a and anti-CD62L in combination with the $M_{187–195}$ tetramer. Numbers represent the percentage of NKG2a^{pos}, CD11a^{hi}/CD62L^{low} CD8$^+$ T cells of total CD8$^+$ T cells ± standard error of the mean (SEM).

[a] Denotes values with a significant difference between day 8 and day 21 in surface expression of the selected marker ($P < 0.01$).

[b] The percentage of CD8$^+$ CD62L^{low} was comparable to the percentage of NKG2a^{pos} CD8$^+$ T cells.

that in time, a fraction of RSV-specific lung T cells lost the capacity to produce IFN-γ in C57BL/6 mice.

Functional inactivation of $M_{187–195}$-specific CD8$^+$ T cells in the lungs

The inability of the $M_{187–195}$-specific CD8$^+$ T cells of the lungs to produce IFN-γ at day 21 after infection was studied in more detail. To confirm that the inactivation was tissue specific and not caused by technical procedures, we compared the $M_{187–195}$-specific CD8$^+$ T cell response in the spleen and lungs at days 8, 21 and 28. According to the report by Chang and Braciale (2002), the effect of CD8$^+$ T cell inactivation is restricted to the lungs. The percentage of $M_{187–195}$-specific CD8$^+$ T cells in the lung parenchyma at day 8 was comparable with the percentage of CD8$^+$ T cells producing IFN-γ after peptide stimulation, 12.1% tetramer-positive versus 12.5% IFN-γ producing CD8$^+$ T cells (Table 3). This was also observed for CD8$^+$ T cells in the spleen at day 8, where 1.4% stained positive with the $M_{187–195}$ tetramer and 1.6% produced IFN-γ after peptide stimulation.

As already observed, there was a discrepancy between $M_{187–195}$ tetramer-specific CD8$^+$ T cells and the number of these cells capable of producing IFN-γ at day 21 from the lung parenchyma. Only 59% of the $M_{187–195}$-specific CD8$^+$ T cells produced IFN-γ, in contrast to the spleen where all $M_{187–195}$-specific CD8$^+$ T cells produced IFN-γ at day 21 after stimulation with the $M_{187–195}$ peptide (Table 3). The difference between $M_{187–195}$ IFN-γ production and $M_{187–195}$ tetramer staining of CD8$^+$ T cells in the lung parenchyma increased even more at day 28 after primary infection. Only 41% of the $M_{187–195}$-specific CD8$^+$ T cells in the lung parenchyma were functional, whereas 83% of these cells in the spleen were functional.

RSV-specific responses in bronchoalveolar lavage

In addition to the immune response in the lung parenchyma, we also studied the RSV-specific response by the pulmonary inflammatory cells in the lung airways 8 and 21 days after RSV infection (Fig. 4). We eluted these cells by bronchoalveolar lavage and examined the activation status of these cells. In the BAL at day 8, about 75% (69% average in the whole group) of the CD8$^+$ T cells could be identified as activated with an NKG2a^{pos}, CD11a^{hi} and CD62L^{low} phenotype (Fig. 4A; Table 2). Of the CD8$^+$ T cells in the BAL, 20% stained positive with the $M_{187–195}$ tetramer, with all the tetramer-positive cells being NKG2a^{pos}, CD11a^{hi} and CD62L^{low} (Fig. 4A; Table 3).

When we applied the same procedure at day 21 post-infection, the majority (81% average in the group; Table 2) of CD8$^+$ T cells remained NKG2a^{pos}. The CD62L expression was low on 86% of the cells. However, the expression of CD11a declined, only 30% (20% average in the group; Table 2) of the CD8$^+$ T cells had the CD11a^{hi}, CD62L^{low} phenotype (Fig. 4B). Despite the low CD11a^{hi} expression by CD8$^+$ T cells, more than 34% of CD8$^+$ T cells stained positive with the $M_{187–195}$ tetramer. These $M_{187–195}$-specific CD8$^+$ T cells predominantly had an NKG2a^{pos}, CD62L^{low} phenotype. Of the $M_{187–195}$-specific CD8$^+$ T cells, only 16.5 ± 3% were CD11a^{hi}. These results suggested that there is an efflux of activated $M_{187–195}$-specific CD8$^+$ T cells from the lung parenchyma into lung airways, where the expression of CD11a is progressively lost. When we looked at the functional responses in the BAL, initially at day 8 after primary infection, the ratio IFN-γ versus tetramer-positive cells was higher than in the lung parenchyma. However, at day 28 the functional inactivation was also found in the BAL (Table 3).

Secondary $M_{187–195}$-specific CD8$^+$ T cell responses in the lungs

The hierarchy of CD8$^+$ T cell immune responses can change after a secondary infection. To test if there was a difference in hierarchy after a secondary RSV infection in the C57BL/6 RSV model, we infected C57BL/6 mice with RSV and 4 weeks later they were intranasally challenged with the same dose of RSV. The lung parenchyma and splenic CD8$^+$ T cells were analyzed 6 days after challenge for their capability to produce IFN-γ after

Fig. 2. Pulmonary CD8$^+$ T cell activation at day 8 after primary RSV infection. Pulmonary lymphocytes were incubated with synthetic peptides (1 μM) for 6 h and IFN-γ production was measured by intracellular staining. (A) The percentages of INF-γ producing CD8$^+$ T cells responding to individual peptides are shown in the upper-right quadrant. One representative FACS plot is shown. Average percentages of the total groups of mice tested and SEM are depicted in Fig. 5C, where the hierarchy of peptide-specific responses at different time points after primary (days 8, 21 and 28) and secondary (day 6) RSV infections are summarized. (B) Relative IFN-γ production after pre-incubation with blocking antibodies or peptide competition. (C) Expression of NKG2a, CD11a and CD62L on pulmonary CD8$^+$ T cells at day 8 p.i. Numbers represent the percentage of live CD8$^+$ T cells in each quadrant. Average percentages and SEM for the total group are summarized in Table 2. (D) Pulmonary lymphocytes 8 days p.i. were stained with $M_{187–195}$ (RSV) or $NP_{366–374}$ (Influenza) tetramer. Numbers represent the percentage of tetramer$^+$ CD8$^+$ T cells. (E) Pulmonary CD8$^+$ T cells were stained with anti-NKG2a, anti-CD11a or anti-CD62L in combination with the $M_{187–195}$ tetramer. Numbers represent the percentage of CD8$^+$ T cells of total pulmonary CD8$^+$ T cells. The pictures shown are representative of four mice per group and two/three individual experiments. The average values of tetramer-positive cells and SEM of the total group can be found in Table 3.

Table 3
C57BL/6 mice were intranasally infected with 2.5×10^6 p.f.u. RSV A2

	Lung parenchyma			Lung airways			Spleen		
	% $Tet^+/CD8^+$	% IFN-$\gamma^+/CD8^+$	% IFN-γ^+/Tet^+	% $Tet^+/CD8^+$	% IFN-$\gamma^+/CD8^+$	% IFN-γ^+/Tet^+	% $Tet^+/CD8^+$	% IFN-$\gamma^+/CD8^+$	% IFN-γ^+/Tet^+
Day 8	12.1 ± 1.5	12.5 ± 0.8	103.2 ± 3.6[a]	20.2 ± 4.0	39.5 ± 4.0	195.5 ± 8.9[a]	1.4 ± 0.2	1.6 ± 0.1	114.3 ± 8.9
Day 21	8.5 ± 1.5	5.0 ± 0.4	58.9 ± 3.9[b]	30.0 ± 3.3	38.9 ± 5.4	128.2 ± 8.7[b]	0.5 ± 0.1	0.6 ± 0.1	128.9 ± 18, ns
Day 28	9.1 ± 1.3	3.5 ± 0.4	41.3 ± 7.2[b]	24.4 ± 2.6	13.6 ± 1.5	55.7 ± 2.5[b]	0.9 ± 0.1	0.7 ± 0.2	83.9 ± 11.6, ns

Lymphocytes obtained from the lung parenchyma, lung airways and spleen (of 4 mice per group from 2 independent experiments) at indicated time points after infection, were stimulated with $M_{187–195}$ peptide for intracellular cytokine staining or stained directly with anti-CD8 and $M_{187–195}$ tetramer. The values represent the percentages of $CD8^+$ T cells staining positive for either IFN-γ or the $M_{187–195}$ tetramer ± standard error of the mean (SEM). Percentages of IFN-γ producing cells among $M_{187–195}$ Tet^+ were calculated by dividing the percentage of IFN-$\gamma^+/CD8^+$ by the percentage of $M_{187–195}$ $Tet^+/CD8^+$ at each time point. ns, not significantly different from day 8.

[a] Denotes significant difference between day 8 lung parenchyma and lung airways ($P < 0.001$).

[b] Denotes values that significantly differ from day 8 ($P < 0.001$).

peptide stimulation. The ICS revealed that $M_{187–195}$ still remained the dominant epitope, with >17% (14% average in the group; Fig. 5C) of the $CD8^+$ T cells producing IFN-γ after stimulation (Fig. 5A). Furthermore, the results showed that the $NP_{360–368}$ epitope was the second dominant epitope with 4.2% IFN-γ-positive $CD8^+$ T cells. There was no clear hierarchy

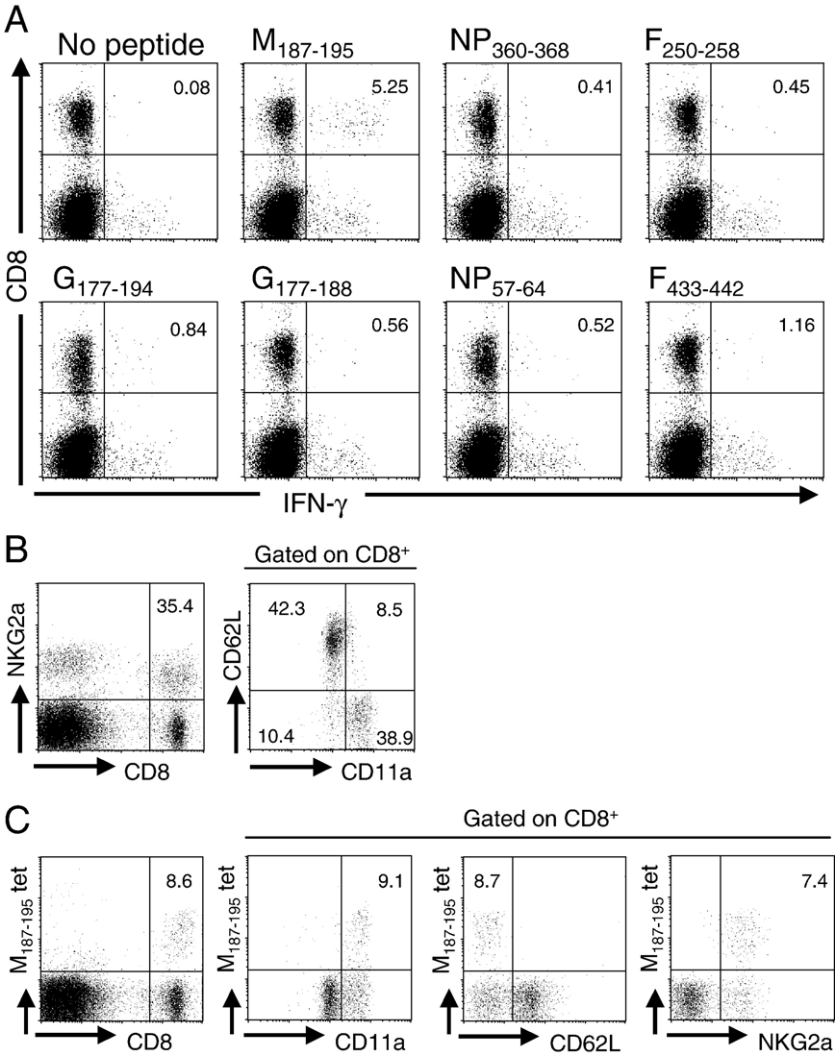

Fig. 3. Pulmonary $CD8^+$ T cell activation at day 21 p.i. (A) Pulmonary lymphocytes were incubated with synthetic peptides and IFN-γ production was measured by intracellular cytokine staining. The percentages of IFN-γ^+ $CD8^+$ T cells out of total live $CD8^+$ T cells are shown in the upper-right quadrant. Average values and SEM of the total group are summarized in Fig. 5C. (B) Expression of NKG2a, CD11a and CD62L on pulmonary $CD8^+$ T cells at day 21 p.i. The numbers represent the percentage of live $CD8^+$ T cells in each quadrant. Average data of the total group are summarized in Table 2. (C) Pulmonary $CD8^+$ T cells were stained with anti-NKG2a, anti-CD11a or anti-CD62L in combination with the $M_{187–195}$ tetramer. Average group values of tetramer-positive cells are given in Table 3. Numbers represent the percentage of $CD8^+$ T cells in the quadrant. Pictures are representative for four individual mice per experiment and two different experiments.

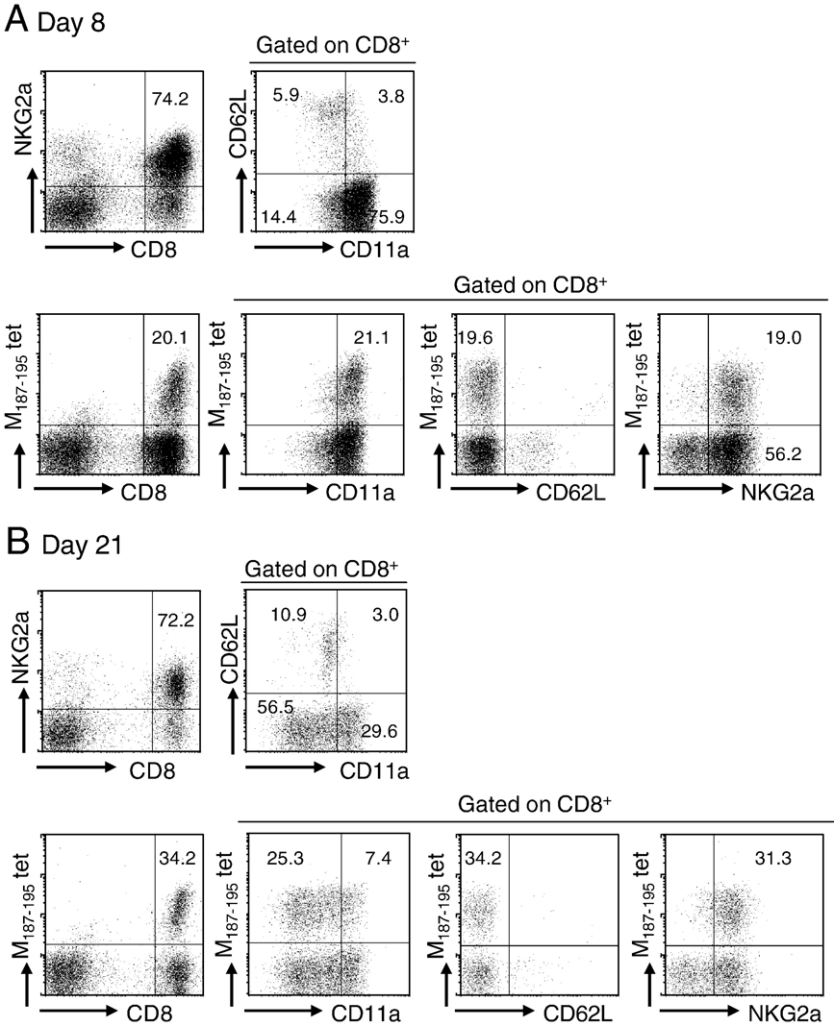

Fig. 4. $CD8^+$ T cell activation in the BAL over time following RSV infection. Expression of activation markers on $CD8^+$ T cells on (A) day 8 p.i. and (B) day 21 p.i. The numbers in the quadrants represent the percentage of cells out of total BAL $CD8^+$ T cell numbers. The pictures shown represent the data from pooled BAL samples of 4 individual mice. The average values and SEM of the fraction of cells expressing activation markers NKG2a and CD11a can be found in Table 2.

between the other epitopes; however, $NP_{57–64}$ and $F_{433–442}$ hardly stimulated any IFN-γ production. Results obtained with control mice undergoing a primary MOCK infection that were challenged 4 weeks later with RSV had 4.3 ± 1.3% of the lung $CD8^+$ T cells producing IFN-γ after $M_{187–195}$ stimulation on day 6 p.i. (Fig. 5B). This showed that during a "primary" infection on day 6, the response against the $M_{187–195}$ epitope was significantly lower compared with 14% IFN-γ production after $M_{187–195}$ stimulation during a recall response. Fig. 5C summarizes the observed $CD8^+$ T cell response (average values of the groups) for the different epitopes at several time points and clearly shows that the secondary response in all the mice was less heterogeneous in the lung parenchyma than the primary response. The substantial responses against the $G_{177–194}$, $NP_{57–64}$ and $F_{433–442}$ epitopes observed during the primary response was not found during the secondary response. In contrast, more $CD8^+$ T cells responded to $NP_{360–368}$ during the secondary response than during the primary response. The boost in the secondary response was not observed in the spleen.

Discussion

$CD8^+$ cytotoxic T lymphocytes play a crucial role in the clearance of RSV infections in humans and in mice. However, most of the studies in the mouse model have been performed in the BALB/c strain, leaving open the question whether important phenomena, such as the functional inactivation of lung $CD8^+$ T cells (Chang and Braciale, 2002), are strain specific or will also occur in mice with different genetic backgrounds. To address such questions, we have identified a panel of H-2^b-restricted $CD8^+$ T cell epitopes derived from the M, NP, F and G proteins of RSV A2. The $M_{187–195}$ epitope was recently reported by Rutigliano et al. (2005). This group discovered only the $M_{187–195}$ epitope, probably because they used as a T cell source, spleen cells derived from C57BL/6 mice after secondary virus infection. In the present paper, we observed an altered epitope hierarchy during primary and secondary RSV-specific T cell responses, whereby the secondary response was indeed dominated by $CD8^+$ T cells responding to the $M_{187–195}$ epitope. Such altered hierarchy in epitope recognition during

primary and secondary responses has also been described for influenza epitopes, where it appeared to be the result of differences in epitope expression by different antigen presenting cell types (Crowe et al., 2003). Most of the identified epitopes contained an H-2D^b binding motif, whereas one peptide NP$_{57–64}$ harbored an H-2K^b binding motif. The G$_{177–194}$ peptide did not contain a clear binding motif for either H-2D^b or H-2K^b, although H-2D^b was found to be the restriction element by means of antibody blocking and peptide competition studies. However, attempts to identify the minimal G epitope were unsuccessful. Contamination with one of the other peptides could be excluded by mass spectrometry (ms) and tandem mass spectrometric sequencing. We are currently working on different approaches to solve the structure of the naturally presented G peptide.

The fact that we found a G-derived peptide that was recognized by CD8$^+$ T cells was interesting because many reports suggested that the G protein is poorly recognized by CD8$^+$ T cells (Bangham et al., 1986; Srikiatkhachorn and Braciale, 1997; Nicholas et al., 1990). In BALB/c mice, the G-specific CD8$^+$ T cell response is clearly absent. This lack of an H-2^b-restricted G-specific CD8$^+$ T cell response has been held responsible for the enhanced CD4$^+$ Th2 response causing lung eosinophilia after vaccination employing the G protein as sole RSV component (Alwan et al., 1994; Srikiatkhachorn and Braciale, 1997). Interestingly, the same priming procedure did not lead to the enhanced disease in C57BL/6 mice (Hussell et al., 1998). The presence or absence of CD8$^+$ T cell responses directed against the G protein in different mouse strains that are relatively resistant to eosinophilic lung disease has not been extensively studied. A possible explanation for the resistance of C57BL/6 mice for enhanced disease after G priming could be the presence of the CD8$^+$ T cell epitope in the G protein. This CD8 epitope might elicit a memory T cell response that could be sufficient to regulate the CD4$^+$ T cell response upon viral challenge.

Eight days after primary intranasal infection with RSV, more than 12% of the CD8$^+$ T cells in the lungs recognized the dominant M$_{187–195}$ peptide. In several reports, it has been shown that NKG2a is up-regulated by CD8$^+$ T cells after contact with antigen and remains expressed long after (Moser et al., 2002). This marker was therefore used as a surrogate activation marker for antiviral CD8$^+$ T cells (Gold et al., 2004; Claassen et al., 2005). We found that at day 8 p.i. about 45% of the CD8$^+$ T cells in the lungs expressed NKG2a. This number is similar for the CD11a^{hi}/CD62L^{low} population. Of the activated pulmonary CD8$^+$ T cells, 25% recognized the M$_{187–195}$ epitope as measured by tetramer staining. Indeed, all M$_{187–195}$-specific cells were CD11a^{hi}/CD62L^{low} and NKG2a^{pos}. Furthermore, the percentage of tetramer-positive cells matched with the percentage of IFN-γ-positive cells. This means that in contrast to CD8$^+$ T cell responses in BALB/c mice all the specific CD8$^+$ T cells in the lungs of C57BL/6 mice were fully functional at day 8 after infection (Chang and Braciale, 2002). If we would assume that also for the other epitopes T cells were fully functional at day 8, this would suggest that the epitopes we have characterized

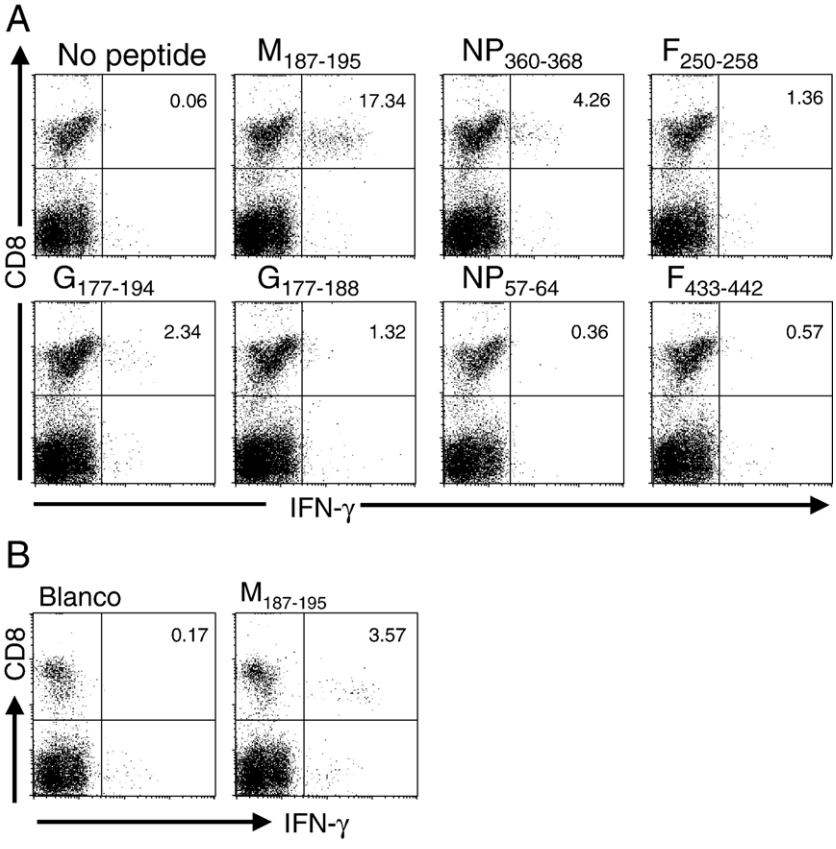

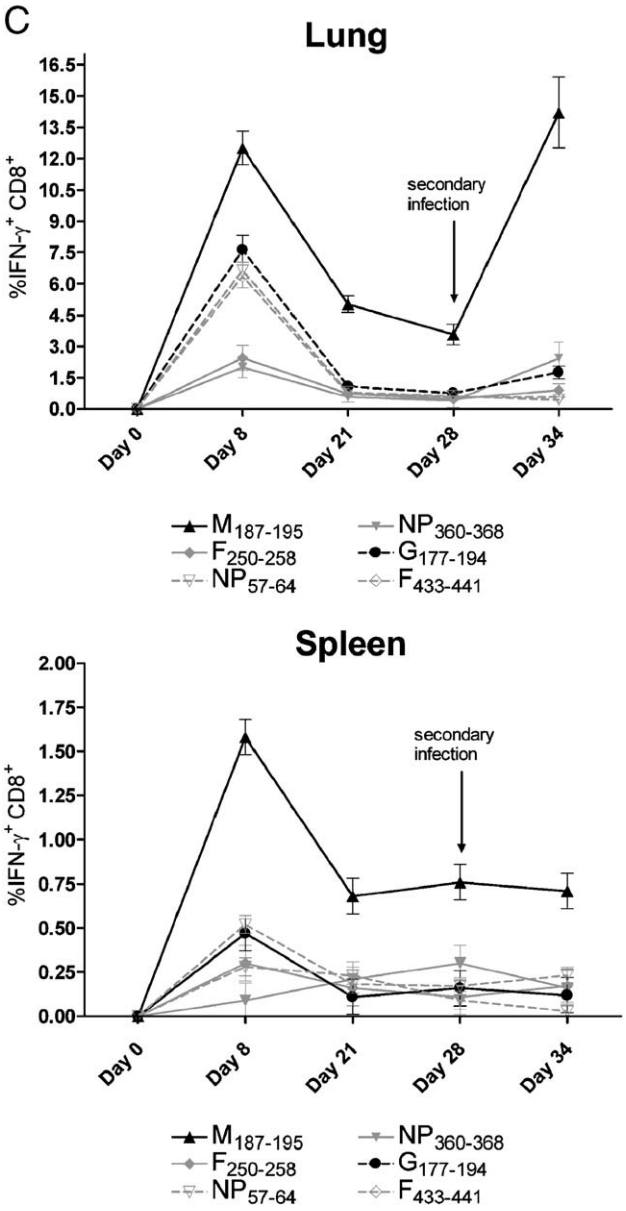

Fig. 5. Epitope hierarchy during RSV-specific $CD8^+$ T cell recall responses in the lung. Pulmonary tissue lymphocytes obtained 6 days after intranasal challenge infection with 2.5×10^6 p.f.u. RSV were in vitro stimulated with synthetic peptides (1 μM) and IFN-γ production was measured using intracellular staining. (A) Primary infection 2.5×10^6 p.f.u. RSV intranasally; (B) primary MOCK infection. The percentages of IFN-γ^+ $CD8^+$ T cells of total $CD8^+$ T cells are shown in the upper-right quadrant. Pictures represent one individual mouse out of 5. (C) Summary of the average fraction of responding $CD8^+$ T cells against the panel of RSV epitopes at different time points after primary and secondary RSV infection. Data from 5 mice of two independent experiments, error bars represent the SEM.

together amount to at least >95% of the virus-specific responses as measured by the total number of $NKG2a^{pos}$, $CD11a^{high}$ and $CD62L^{low}$ $CD8^+$ T cells.

The memory response against RSV is usually incomplete and individuals can be re-infected within a short period with the same strain (Hall et al., 1991). One possible explanation for the inefficient induction of T cell memory might be the $CD8^+$ T cell inactivation that occurs in RSV-infected lungs that was observed in BALB/c mice (Chang and Braciale, 2002). When we studied the transition from effector to early memory phase at days 21 and 28 post-infection in C57BL/6 mice, we found that the decline in IFN-γ producing $CD8^+$ T cells was greater than the decline in activated $CD8^+$ T cells defined as $NKG2a^{pos}$, $CD11a^{hi}$ and $CD62L^{low}$. Tetramer staining at these time points showed that $M_{187–195}$ $CD8^+$ T cells were present, but they started to lose their functional response, like it was described for $CD8^+$ T cell responses in the lungs of RSV-infected BALB/c mice. The effect of functional inactivation on viral clearance is yet to be determined. However, we showed that upon secondary infection to RSV a robust recall response could be measured against the matrix epitope. These matrix-specific T cells could potentially contribute to viral clearance.

Functional inactivation has also been described for other viruses from the Paramyxoviridae family (Gray et al., 2005;

Chang and Braciale, 2002; Claassen et al., 2005). The fact that the decrease of function started later during primary RSV infection in C57BL/6 mice might be explained by a lower replication of RSV in the lungs of C57BL/6 mice compared with BALB/c mice. Interestingly, Ostler et al. found a more delayed decrease in the number of functional T cells in RSV-infected BALB/c mice lungs than Chang et al. (2001), which may be related to differences in levels of virus replication reached in the experiments performed by both groups (Ostler and Ehl, 2002; Chang and Braciale, 2002). Furthermore, our observation that functional inactivation increases over time is in agreement with findings for RSV, pneumonia virus of mice (PVM) and simian virus 5 (SV5) infections in BALB/c mice (Chang and Braciale, 2002; Gray et al., 2005; Claassen et al., 2005).

In contrast to the lower numbers of epitope-specific cells detected with the intracellular cytokine staining assay compared to the direct tetramer staining in the lung parenchyma, we found the opposite in the BAL, that is, higher numbers of IFN-γ producing cells than tetramer-positive cells (Table 3). A possible explanation for this observation could be that in the BAL $CD8^+$ T cells had been recently exposed to antigen, which leads to initial T cell receptor down-regulation followed by re-expression. As a result, tetramer staining may be ineffective because the distribution of the T cell receptors on the cell surface may be diffused in the early phase of re-expression although the functional responses triggered by antigenic peptides are effective (Drake et al., 2005).

In conclusion, we have identified a panel of MHC class I epitopes from the F, M, NP and G protein of RSV A2. The responses against the dominant $M_{187–195}$ are fully functional at day 8 during a primary infection. However, at later time points, part of the cells become functionally inactive when triggered via the T cell receptor with cognate antigen. The number of dysfunctional cells increased over time, which was in agreement with observations made for other members of the Paramyxoviridae family. However, our data also suggest that the kinetics of inactivation differs between C57BL/6 and BALB/c mice, and it is tempting to speculate that this may be driven by different viral loads.

Materials and methods

Mice

Pathogen-free 6- to 8-week-old female C57BL/6cjo were purchased from Charles River Nederland (Maastricht, The Netherlands). The mouse study protocols were approved by the Animal Ethics Committee of the Medical Faculty of the Utrecht University.

Viruses and infections

RSV A2 strain was grown in HEp-2 cells, purified by PEG precipitation and stored in liquid nitrogen in 25% sucrose in PBS. Mice were lightly anesthetized with ether and intranasally infected with 2.5×10^6 p.f.u. RSV in a volume of 50 μl or with 1 hemagglutination unit influenza A/NT/60/68 in 50 μl diluted in PBS with 10% sucrose.

Peptides

The RSV proteome with the exception of the L protein was screened for predicted epitopes for the $H\text{-}2D^b$ and the $H\text{-}2K^b$ alleles, using the algorithms for epitope prediction of the SYFPEITHI (http://www.syfpeithi.de) (Rammensee et al., 1999) and BIMAS Web sites (http://www.bimas.dcrt.nih.gov/molbio/hla_bind/) (Parker et al., 1994). Only predicted epitopes present in the top ten in both databases were synthesized and screened (Table 1). All peptides were synthesized by standard solid-phase Fmoc chemistry. In recent work, we had prepared a set of overlapping 18 amino acid long peptide amides that overlapped by 12 residues, spanning the entire F protein (van Bleek et al., 2003).

Tissue sampling

Mice were sacrificed by i.p. injection of 300 μl pentobarbital. Effector cells from the lung airways were obtained by performing a bronchoalveolar lavage (BAL) with 5 × 1 ml of 0.15 M NaCl. Prior to removal, the lungs were perfused with PBS containing 100 U/ml heparin. Lungs were sliced to 1 × 1 mm pieces that were incubated for 30 min at 37 °C with collagenase (2.4 mg/ml; Roche Applied Science, Basel, Switzerland) and DNAase (1 mg/ml; Roche Applied Science, Basel, Switzerland). Single cell suspensions were prepared from the pre-treated lungs and spleen by processing the tissue trough cell strainers. Spleen cells were depleted of erythrocytes by treatment with buffered ammonium chloride solution.

Elispot assay

The IFN-γ Elispot assay was performed on splenocytes of mice obtained 8 days after primary infection, using the mouse IFN-γ Elispot pair (U-cytech, Utrecht, The Netherlands) and Multiscreen-IP filter plates (Millipore, Billerica, MA) according to the manufacturers instructions. Cells were stimulated in 200 μl IMDM (Gibco, Invitrogen) containing 10% FCS, penicillin/streptomycin and 50 μM 2-mercapto-ethanol with 10 μg/ml peptide for 24 h at 37 °C, 5% CO_2.

Intracellular cytokine staining (ICS)

For ICS analysis, single cell suspensions of BAL, lung and spleen cells (10^6) were stimulated for 6 h at 37 °C, 5% CO_2 with 1 μg/ml peptide in 200 μl IMDM (Gibco, Invitrogen) containing 10% FCS, penicillin/streptomycin and 50 μM 2-mercapto-ethanol. Brefeldin-A 10 μg/ml (Sigma, St. Louis, MO) was added for the duration of the stimulation to facilitate intracellular accumulation of cytokines. To determine the restriction element for the $G_{177–194}$ peptides, we incubated lung cells with blocking antibodies to $H\text{-}2D^b$ or H-

$2K^b$, or with the Influenza peptide $NP_{366–374}$ (H-$2D^b$) or VSV peptide $NP_{52–59}$ (H-$2K^b$) for 30 min at 37 °C, 5% CO_2, before the $G_{177–194}$ peptide from RSV was added. After 5 h of stimulation with the $G_{177–194}$ peptide, the cells were washed with PBS containing 2% FCS, 2 mM EDTA and 0.02% NaN_3 (FACS buffer) and surface stained for flow cytometric analysis. Before intracellular staining, cells were fixed and permeabilized with CytoFix/CytoPerm solution and Perm/Wash buffer (BD Pharmingen, San Diego, CA) according to instructions of the manufacturer.

Flow cytometric analysis of $CD8^+$ T cells

MHC class I-peptide tetramers were produced as described (Haanen et al., 1999). Freshly isolated BAL, lung or spleen lymphocytes were stained in FACS buffer, using fluorochrome-conjugated antibodies and $M_{187–195}$ RSV- and $NP_{366–374}$ Influenza-MHC class I tetramers. The antibodies, anti-CD8 (clone 53–6.7), anti-CD11a (2D7), anti-CD62L (clone MEL-14) and anti-NKG2a (20D5) were used for cell surface staining. For intracellular IFN-γ staining, we used the rat-anti-mouse IFN-γ FITC (clone XMG 1.2). All antibodies were purchased from BD Pharmingen (San Diego, CA). Stained samples were acquired on a FACSCalibur flowcytometer (BD, San Diego, CA). Data were analyzed using CellQuest software (BD, San Diego, CA).

Statistical analysis

Data were analyzed for statistical significance using a Students *t* test. Data are expressed as the mean ± standard error of the mean (SEM). A P value <0.05 was taken as the level of significance.

Acknowledgments

We thank Hugo Meiring of the Laboratory of Analytical Chemistry, Netherlands Vaccine Institute, Bilthoven, and Dr. Berthil Prinsen of the Department of Metabolic and Endocrine Diseases, University Medical Center, Utrecht, for assistance with mass spectrometry experiments. Dr. Kiki Tesselaar of the Department of Immunology, University Medical Center, Utrecht, kindly provided the influenza tetramer. This work was supported by grant No. OZF-02-004 from the Wilhelmina Research Fund.

References

Alwan, W.H., Kozlowska, W.J., Openshaw, P.J., 1994. Distinct types of lung disease caused by functional subsets of antiviral T cells. J. Exp. Med. 179, 81–89.

Bangham, C.R., Openshaw, P.J., Ball, L.A., King, A.M., Wertz, G.W., Askonas, B.A., 1986. Human and murine cytotoxic T cells specific to respiratory syncytial virus recognize the viral nucleoprotein (N), but not the major glycoprotein (G), expressed by vaccinia virus recombinants. J. Immunol. 137, 3973–3977.

Bont, L., Steijn, M., Van Aalderen, W.M., Brus, F., Th Draaisma, J.M., Diemen-Steenvoorde, R.A., Pekelharing-Berghuis, M., Kimpen, J.L., 2004. Seasonality of long term wheezing following respiratory syncytial virus lower respiratory tract infection. Thorax 59, 512–516.

Chang, J., Braciale, T.J., 2002. Respiratory syncytial virus infection suppresses lung $CD8^+$ T-cell effector activity and peripheral $CD8^+$ T-cell memory in the respiratory tract. Nat. Med. 8, 54–60.

Chang, J., Srikiatkhachorn, A., Braciale, T.J., 2001. Visualization and characterization of respiratory syncytial virus F-specific CD8(+) T cells during experimental virus infection. J. Immunol. 8, 4254–4260.

Chin, J., Magoffin, R.L., Shearer, L.A., Schieble, J.H., Lennette, E.H., 1969. Field evaluation of a respiratory syncytial virus vaccine and a trivalent parainfluenza virus vaccine in a pediatric population. Am. J. Epidemiol. 89, 449–463.

Claassen, E.A., van der Kant, P.A., Rychnavska, Z.S., van Bleek, G.M., Easton, A.J., van der Most, R.G., 2005. Activation and inactivation of antiviral CD8 T cell responses during murine *Pneumovirus* infection. J. Immunol. 175, 6597–6604.

Connors, M., Kulkarni, A.B., Firestone, C.Y., Holmes, K.L., Morse III, H.C., Sotnikov, A.V., Murphy, B.R., 1992. Pulmonary histopathology induced by respiratory syncytial virus (RSV) challenge of formalin-inactivated RSV-immunized BALB/c mice is abrogated by depletion of $CD4^+$ T cells. J. Virol. 66, 7444–7451.

Crowe, S.R., Turner, S.J., Miller, S.C., Roberts, A.D., Rappolo, R.A., Doherty, P.C., Ely, K.H., Woodland, D.L., 2003. Differential antigen presentation regulates the changing patterns of $CD8^+$ T cell immunodominance in primary and secondary influenza virus infections. J. Exp. Med. 198, 399–410.

de Graaff, P.M., de Jong, E.C., van Capel, T.M., van Dijk, M.E., Roholl, P.J., Boes, J., Luytjes, W., Kimpen, J.L., van Bleek, G.M., 2005. Respiratory syncytial virus infection of monocyte-derived dendritic cells decreases their capacity to activate CD4 T cells. J. Immunol. 175, 5904–5911.

Drake III, D.R., Ream, R.M., Lawrence, C.W., Braciale, T.J., 2005. Transient loss of MHC class I tetramer binding after $CD8^+$ T cell activation reflects altered T cell effector function. J. Immunol. 175, 1507–1515.

Falsey, A.R., Hennessey, P.A., Formica, M.A., Cox, C., Walsh, E.E., 2005. Respiratory syncytial virus infection in elderly and high-risk adults. N. Engl. J. Med. 352, 1749–1759.

Gold, M.C., Munks, M.W., Wagner, M., McMahon, C.W., Kelly, A., Kavanagh, D.G., Slifka, M.K., Koszinowski, U.H., Raulet, D.H., Hill, A.B., 2004. Murine cytomegalovirus interference with antigen presentation has little effect on the size or the effector memory phenotype of the CD8 T cell response. J. Immunol. 172, 6944–6953.

Gray, P.M., Arimilli, S., Palmer, E.M., Parks, G.D., Alexander-Miller, M.A., 2005. Altered function in $CD8^+$ T cells following paramyxovirus infection of the respiratory tract. J. Virol. 79, 3339–3349.

Guinazu, N., Pellegrini, A., Giordanengo, L., Aoki, M.P., Rivarola, H.W., Cano, R., Rodrigues, M.M., Gea, S., 2004. Immune response to a major *Trypanosoma cruzi* antigen, cruzipain, is differentially modulated in C57BL/6 and BALB/c mice. Microbes Infect. 6, 1250–1258.

Haanen, J.B., Toebes, M., Cordaro, T.A., Wolkers, M.C., Kruisbeek, A.M., Schumacher, T.N., 1999. Systemic T cell expansion during localized viral infection. Eur. J. Immunol. 29, 1168–1174.

Hall, C.B., Walsh, E.E., Long, C.E., Schnabel, K.C., 1991. Immunity to and frequency of reinfection with respiratory syncytial virus. J. Infect. Dis. 163, 693–698.

Hussell, T., Baldwin, C.J., O'Garra, A., Openshaw, P.J., 1997. $CD8^+$ T cells control Th2-driven pathology during pulmonary respiratory syncytial virus infection. Eur. J. Immunol. 27, 3341–3349.

Hussell, T., Georgiou, A., Sparer, T.E., Matthews, S., Pala, P., Openshaw, P.J., 1998. Host genetic determinants of vaccine-induced eosinophilia during respiratory syncytial virus infection. J. Immunol. 161, 6215–6222.

Kim, H.W., Canchola, J.G., Brandt, C.D., Pyles, G., Chanock, R.M., Jensen, K., Parrott, R.H., 1969. Respiratory syncytial virus disease in infants despite prior administration of antigenic inactivated vaccine. Am. J. Epidemiol. 89, 422–434.

Lenzo, J.C., Mansfield, J.P., Sivamoorthy, S., Cull, V.S., James, C.M., 2003. Cytokine expression in murine cytomegalovirus-induced myocarditis: modulation with interferon-alpha therapy. Cell. Immunol. 223, 77–86.

Moser, J.M., Gibbs, J., Jensen, P.E., Lukacher, A.E., 2002. CD94-NKG2A receptors regulate antiviral CD8(+) T cell responses. Nat. Immunol. 3, 189–195.

Nicholas, J.A., Rubino, K.L., Levely, M.E., Adams, E.G., Collins, P.L., 1990. Cytolytic T-lymphocyte responses to respiratory syncytial virus: effector cell phenotype and target proteins. J. Virol. 64, 4232–4241.

Ostler, T., Ehl, S., 2002. Pulmonary T cells induced by respiratory syncytial virus are functional and can make an important contribution to long-lived protective immunity. Eur. J. Immunol. 32, 2562–2569.

Parker, K.C., Bednarek, M.A., Coligan, J.E., 1994. Scheme for ranking potential HLA-A2 binding peptides based on independent binding of individual peptide side-chains. J. Immunol. 152, 163–175.

Preston, F.M., Beier, P.L., Pope, J.H., 1995. Identification of the respiratory syncytial virus-induced immunosuppressive factor produced by human peripheral blood mononuclear cells in vitro as interferon-alpha. J. Infect. Dis. 172, 919–926.

Prince, G.A., Horswood, R.L., Berndt, J., Suffin, S.C., Chanock, R.M., 1979. Respiratory syncytial virus infection in inbred mice. Infect. Immun. 26, 764–766.

Rammensee, H., Bachmann, J., Emmerich, N.P., Bachor, O.A., Stevanovic, S., 1999. SYFPEITHI: database for MHC ligands and peptide motifs. Immunogenetics 50, 213–219.

Rutigliano, J.A., Rock, M.T., Johnson, A.K., Crowe Jr., J.E., Graham, B.S., 2005. Identification of an H-2D(b)-restricted $CD8^+$ cytotoxic T lymphocyte epitope in the matrix protein of respiratory syncytial virus. Virology 337, 335–343.

Sacks, D., Noben-Trauth, N., 2002. The immunology of susceptibility and resistance to *Leishmania* major in mice. Nat. Rev., Immunol. 2, 845–858.

Salkind, A.R., McCarthy, D.O., Nichols, J.E., Domurat, F.M., Walsh, E.E., Roberts Jr., N.J., 1991. Interleukin-1-inhibitor activity induced by respiratory syncytial virus: abrogation of virus-specific and alternate human lymphocyte proliferative responses. J. Infect. Dis. 163, 71–77.

Schlender, J., Walliser, G., Fricke, J., Conzelmann, K.K., 2002. Respiratory syncytial virus fusion protein mediates inhibition of mitogen-induced T-cell proliferation by contact. J. Virol. 76, 1163–1170.

Srikiatkhachorn, A., Braciale, T.J., 1997. Virus-specific $CD8^+$ T lymphocytes downregulate T helper cell type 2 cytokine secretion and pulmonary eosinophilia during experimental murine respiratory syncytial virus infection. J. Exp. Med. 186, 421–432.

Stark, J.M., McDowell, S.A., Koenigsknecht, V., Prows, D.R., Leikauf, J.E., Le Vine, A.M., Leikauf, G.D., 2002. Genetic susceptibility to respiratory syncytial virus infection in inbred mice. J. Med. Virol. 67, 92–100.

van Bleek, G.M., Poelen, M.C., van der, M.R., Brugghe, H.F., Timmermans, H.A., Boog, C.J., Hoogerhout, P., Otten, H.G., van Els, C.A., 2003. Identification of immunodominant epitopes derived from the respiratory syncytial virus fusion protein that are recognized by human CD4 T cells. J. Virol. 77, 980–988.

Waris, M.E., Tsou, C., Erdman, D.D., Zaki, S.R., Anderson, L.J., 1996. Respiratory syncytial virus infection in BALB/c mice previously immunized with formalin-inactivated virus induces enhanced pulmonary inflammatory response with a predominant Th2-like cytokine pattern. J. Virol. 70, 2852–2860.